J Biomol NMR (2013) 55:147–155
DOI 10.1007/s10858-013-9710-5

COMMUNICATION

Yeast-expressed human membrane protein aquaporin-1 yields excellent resolution of solid-state MAS NMR spectra

Sanaz Emami · Ying Fan · Rachel Munro · Vladimir Ladizhansky · Leonid S. Brown

Received: 14 December 2012 / Accepted: 15 January 2013 / Published online: 24 January 2013

Abstract One of the biggest challenges in solid-state NMR studies of membrane proteins is to obtain a homogeneous natively folded sample giving high spectral resolution sufficient for structural studies. Eukaryotic membrane proteins are especially difficult and expensive targets in this respect. Methylotrophic yeast *Pichia pastoris* is a reliable producer of eukaryotic membrane proteins for crystallography and a promising economical source of isotopically labeled proteins for NMR. We show that eukaryotic membrane protein human aquaporin 1 can be doubly ($^{13}C/^{15}N$) isotopically labeled in this system and functionally reconstituted into phospholipids, giving excellent resolution of solid-state magic angle spinning NMR spectra.

Keywords Eukaryotic membrane proteins · Solid-state NMR · Magic angle spinning · Human aquaporin-1 · *Pichia pastoris* · Spectral resolution

It is a general consensus that, despite a number of recent breakthroughs, the pace of progress in structural studies of membrane proteins lags behind that of proteins in general (White 2009). The need for new methodologies in this field is obvious, and novel techniques of solution and solid-state (SS) NMR are being applied to studies of structure and dynamics of membrane proteins (Li et al. 2008; Barnes et al. 2008; Kim et al. 2009; McDermott 2009; Renault et al. 2010; Tapaneeyakorn et al. 2011; Marassi et al. 2011; Reckel et al. 2011; Gautier and Nietlispach 2012; Hong et al. 2012; Qureshi and Goto 2012). The key prerequisite of any successful NMR study is a production of natively folded, isotopically labeled, structurally homogeneous protein, which requires robust overexpression and functional reconstitution into a membrane-like environment. Eukaryotic membrane proteins are particularly challenging targets, in view of the difficulties of achieving their high expression levels in combination with the native fold and post-translational modifications in heterologous systems. Thus, much effort has been spent on experimentation with various expression methods and suitable membrane mimics (Kim et al. 2009; Takahashi and Shimada 2010; Goncalves et al. 2010; Reckel et al. 2010; Warschawski et al. 2011; Tapaneeyakorn et al. 2011).

Expression in *Escherichia coli* remains the easiest and the cheapest method of production of eukaryotic membrane proteins for NMR. Even though it yielded several structures (Hiller et al. 2008; Berardi et al. 2011; Verardi et al. 2011; Park et al. 2012) and some promising samples (Berger et al. 2010), the problems of non-native fold or poor expression are often encountered. The alternatives such as cell-free expression, as well as mammalian and insect cell cultures, used to be very costly, considering that milligram quantities of uniformly labeled protein are required, but the progress in these areas is obvious (Ratnala 2006; Makino et al. 2010; Egorova-Zachernyuk et al. 2011; Isaksson et al. 2012). These techniques yet have to produce full NMR structures of eukaryotic membrane proteins, even though there are recent examples of backbone structure determination (Klammt et al. 2012) and experiments based on specific labeling (Werner et al. 2008; Ahuja et al. 2009). An alternative, which has not yet been extensively utilized for isotopic labeling of membrane proteins is expression in yeast, especially the metylotrophic yeast

S. Emami · Y. Fan · R. Munro · V. Ladizhansky · L. S. Brown (✉)
Departments of Physics, and Biophysics Interdepartmental Group, University of Guelph, 50 Stone Road East, Guelph, ON N1G 2W1, Canada
e-mail: lebrown@uoguelph.ca

Pichia pastoris (Pickford and O'Leary 2004; Sugiki et al. 2012), despite the fact that it has been actively explored for production of eukaryotic membrane proteins for crystallographic studies (Lundstrom et al. 2006; Oberg et al. 2009; Asada et al. 2011; Singh et al. 2012; Bornert et al. 2012).

Pichia pastoris is a promising candidate for isotopic labeling of eukaryotic membrane proteins due to the powerful combination of two factors. First, *Pichia* showed its promise in NMR studies of soluble proteins, and the protocols for their efficient and inexpensive isotopic labeling are well developed (Wood and Komives 1999; Morgan et al. 2000; Rodriguez and Krishna 2001; Pickford and O'Leary 2004; Sugiki et al. 2012). Second, there is a vast literature on crystallographic studies of *Pichia*-expressed mammalian membrane proteins in their functional forms, including a number of X-ray structures of channels, transporters, and G-protein coupled receptors (GPCRs) (Long et al. 2005; Horsefield et al. 2008; Tao et al. 2009; Ho et al. 2009; Aller et al. 2009; Shimamura et al. 2011; Hino et al. 2012). Even though it seems that amalgamation of these two streams of knowledge should have produced a number of membrane protein samples suitable for high-resolution NMR, such examples are still very rare.

Recently, we adapted and optimized protocols developed for isotope labeling of soluble proteins in *Pichia* (Rodriguez and Krishna 2001; Pickford and O'Leary 2004) for eukaryotic seven-transmembrane-helical (7TM) protein, fungal rhodopsin from *Leptosphaeria maculans* (LR) (Waschuk et al. 2005). Doubly ($^{13}C/^{15}N$) isotopically labeled LR was expressed in shake-flasks with the yield exceeding 5 mg of purified protein per liter and, upon functional reconstitution into synthetic lipids, gave high spectral resolution in magic angle spinning (MAS) SSNMR, comparable to that obtained for bacterial homologs produced in *E. coli* (Fan et al. 2011). In the present work, we extend this protocol to the double-isotope-labeling and functional lipid reconstitution of mammalian multi-spanning membrane protein, human aquaporin 1 (hAQP1), which yielded MAS SSNMR spectra of an exceptional resolution amenable to the detailed structural analysis.

Human aquaporin 1 is a tetrameric α-helical integral membrane protein (with monomer molecular weight of ~28.5 kDa), which is expressed in multiple tissues and mainly serves as a selective water channel, even though other physiological functions have been suggested (Agre et al. 2002; Yool 2007; Musa-Aziz et al. 2009). Upregulation and mutations of hAQP1 have been implicated in several human diseases and its pharmacology is being actively explored (Yool et al. 2010; Seeliger et al. 2012). Medium-resolution structure of hAQP1 is known from the electron diffraction studies (Murata et al. 2000; Ren et al. 2001; de Groot et al. 2001), and even higher resolution X-ray structure of highly homologous bovine aquaporin is available (Sui et al. 2001). Based on this structural information and computational approaches (de Groot et al. 2003; Chen et al. 2007), the basic mechanisms of water permeability and selectivity are well understood, while regulation and pharmacology of hAQP1 are less established. SSNMR gives an opportunity to study these aspects in the native-like lipid environment at non-cryogenic temperatures, which provides the motivation for this isotope-labeling trial.

Previously, expression of hAQP1 in *P. pastoris* was shown to produce exceptionally high yields in shake-flasks and especially in fermenters, and has been thoroughly optimized (Nyblom et al. 2007; Oberg et al. 2011; Norden et al. 2011). We used the expression plasmid developed earlier elsewhere (Nyblom et al. 2007), while the isotope labeling protocol for hAQP1 in *P. pastoris* mainly followed our protocol developed for *Leptosphaeria* rhodopsin (LR) (Fan et al. 2011) with some modifications. The modifications introduced for hAQP1 mainly relate to the protein solubilization and reconstitution steps, similar to those employed earlier (Nyblom et al. 2007).

The expression vector pPICZB-hAQP1-Myc-His6 (kindly provided by Frederick Öberg and Kristina Hedfalk, Göteborg University, Sweden) encodes full-length hAQP1 with a C-terminal Myc and 6xHis tags and allows for selection of the transformants based on resistance to zeocin. The plasmid was linearized using PmeI (New England Biolabs), desalted by the QIAquick nucleotide removal kit (Qiagen), and transformed into protease-deficient *P. pastoris* strain SMD1168H (Invitrogen) by electroporation (Micro-Pulser, Bio-Rad) as described previously (Fan et al. 2011). The transformants were grown on yeast peptone dextrose sorbitol (YPDS) plates containing two different concentrations of zeocin (Cedarlane, 100 and 500 μg/ml). To screen the transformants for the highest level of hAQP1 production, eight colonies were selected for small-scale growth. The colonies were inoculated in 5 mL buffered minimal dextrose (BMD) media and grown in shake-flasks at 300 rpm and 30 °C overnight. An additional 20 mL of BMD media was added to the cultures when OD_{600} exceeded 2 and the cultures were shaken at 300 rpm and 30 °C for 24 h, or until OD_{600} reached 10. The cells were collected by centrifugation at 1,500 × *g*, 4 °C for 10 min, resuspended in 25 mL buffered minimal methanol (BMM) media in 250 mL flasks, and grown for 24 h at 240 rpm and 28 °C. The cells were harvested and resuspended in cell resuspension buffer (CRB) containing 20 mM Tris–HCl, pH 7.6, 100 mM NaCl, 0.5 mM EDTA, and 5 % (w/v) glycerol (Nyblom et al. 2007). To digest the cell walls, 15 mg of lyticase (from *Arthrobacter luteus*, Sigma) were added to the pellets and incubated with slow shaking for 3 h at room temperature.

The cells were centrifuged at 1,500×*g* for 5 min at 4 °C, and immediately resuspended in one pellet volume of CRB buffer, the same volume of ice-cold acid-washed glass beads (Fisher, 420–600 μm diameter) was added, and the cells were disrupted using vigorous vortex mixing. The cell debris were removed by centrifugation at 700×*g* for 5 min at 4 °C and the cell lysate was collected. Vortexing and centrifugation were repeated 8 times to achieve complete breakage of the cells. All cell supernatants containing the membrane fraction were combined and centrifuged at 40,000×*g* for 30 min at 4 °C. The relative hAQP1 content of these membranes was monitored by immunoblotting (using anti-His_6 primary antibody, Clontech and anti-mouse IgG HRP Conjugate secondary antibody, Bio-Rad) and the colony giving the most intense band corresponding to the His-tagged protein (MW about 30 kDa) was chosen for the large-scale growth and isotope labeling. Before proceeding with the large-scale expression, we performed additional optimization of the post-induction growth length (the time between transfer to BMM and harvesting) in the small-scale cultures, using a colony with the highest level of hAQP1 expression. The cells were harvested after 6, 12, 24, 36, and 44 h after the induction (additional 0.5 % methanol was added after 24 h) and the level of expression was monitored by immunoblotting. As a result of this screening, we found that the best time for harvesting the cells is 24 h. Longer incubation did not produce appreciable increase in the hAQP1 yield but required the addition of extra methanol. In fact, the amount of hAQP1 substantially decreased upon prolonged induction (barely detectable at 44 h). Similar trends were observed earlier for puroindoline-a (Issaly et al. 2001) and for LR, but the peak yield for LR was shifted to about 40 h (Fan et al. 2011), stressing the need for thorough individual screening for each protein.

For the large-scale expression and isotope labeling of hAQP1, the best producing colony was used to inoculate 50 mL of ^{13}C,^{15}N-BMD containing 0.8 % $(^{15}NH_4)_2SO_4$ and 0.5 % ^{13}C glucose (Cambridge Isotope Laboratories) in a 250 mL baffled flask. The cells were grown at 300 rpm and 30 °C for 18–24 h and transferred to a 2 L baffled flask with an additional 200 mL of isotope-labeled BMD. The cells were then shaken at 275 rpm and 29 °C for 18–24 h before being spun down at 1,500×*g* at 4 °C for 10 min. The cells were resuspended in 1 L of ^{13}C,^{15}N-BMM (0.5 % ^{13}C-methanol (Cambridge Isotope Laboratories) and 0.8 % $(^{15}NH_4)_2SO_4$) in a sterile 2.8 L flask and grown for 24 h at 240 rpm and 28 °C. The cells were collected by centrifugation at 1,500×*g*, 4 °C for 10 min and washed twice with MilliQ water before storing the pellet at −20 °C for later use. The cells were broken and the membrane fraction was collected as described above, and the total protein concentration was determined by Bradford assay with bovine serum albumin standard (Bio-Rad DC Protein assay).

hAQP1 was solubilized by resuspending the membrane fraction from 1 L culture in 60 mL of solubilization buffer (20 mM Tris–HCl pH 8.0, 100 mM NaCl, 20 % glycerol, 10 mM imidazole, protease inhibitor cocktail (for general use, Sigma), and 5 % *n*-octyl-β-D-glucopyranoside (β-OG, Fisher)) (Nyblom et al. 2007). The mixture was stirred at 4 °C for 2 h and unsolubilized material was removed by centrifugation at 160,000×*g* for 30 min at 4 °C. The supernatant containing solubilized hAQP1 was incubated with 2 mL of Ni^{2+}-NTA resin (Qiagen) for 3 h at 4 °C. The resin was placed in a column and washed with washing buffer (30 mM imidazole, 20 mM Tris–HCl pH 8.0, 100 mM NaCl, 20 % glycerol, protease inhibitor cocktail, 1 % β-OG). Next, hAQP1 was eluted using elution buffer with increasing concentrations of imidazole (150 mM, 250 mM, or 500 mM in 20 mM Tris–HCl pH 8.0, 100 mM NaCl, 20 % glycerol, protease inhibitor cocktail, 1 % β-OG) (Nyblom et al. 2007). Immunoblotting was used to verify hAQP1 presence throughout the purification process and the completeness of binding to the resin. The final yield of purified hAQP1 was estimated by Bradford assay as well as by UV–Vis spectroscopy (Cary 50, Varian) after the removal of imidazole, using estimated absorbance of 0.1 % (= 1 g/L) hAQP1 of 0.944 (PROTPARAM), as well as by the amplitudes of FTIR and NMR signals after lipid reconstitution (see below). The total yield of ~6 mg of isotope-labeled protein per liter of culture is similar to that obtained for LR (Fan et al. 2011) and represents very economical protocol, considering that no second addition of ^{13}C-methanol was required. The purity of the final preparation was assessed by Coumassie SDS-PAGE and MALDI TOF mass spectrometry (University of Guelph Advanced Analysis Centre). Mass spectra contained two peaks corresponding to approximate molecular weights of 31,257 and 28,468 Da. The main peak at 31,257 ± 10 Da is close to that expected for sodium adduct of non-glycosylated natural abundance His- and Myc- tagged hAQP1 (MW of 31,205 Da estimated from PROTPARAM). This suggests that hAQP1 expressed in *P. pastoris* does not undergo appreciable glycosylation, consistent with the lack of sugar signals in carbon NMR spectra (see below), and similar to the situation with fungal rhodopsins (Fan et al. 2011). It should be noted that hAQP1 expressed in *Saccharomyces cerevisiae* was not glycosylated either, unlike the native protein from erythrocytes (Laize et al. 1997). An additional minor mass peak of 28,468 Da most probably corresponds to the post-translationally N-terminally truncated species. The corresponding band could be also observed on Western blots, but only if high concentrations of hAQP1 were used (not shown), and was also noted before (Nyblom et al. 2007; Oberg et al. 2009).

To perform lipid reconstitution of hAQP1 for solid-state NMR, the lipid stock (egg PC:brain PS = 9:1 w/w, Avanti

lipids) was prepared as described earlier (Fan et al. 2011), in 50 mM KH_2PO_4, 100 mM NaCl, pH 7.5, at ~11 mg/mL. Purified hAQP1 in 30 mL of elution buffer at 0.2 mg/mL concentration was concentrated to 5 mL volume with concurrent removal of imidazole (Amicon centrifugal concentrator, 10 kDa cut-off, Fisher) and mixed with the lipid stock at the protein/lipid ratio of 2 (w/w) (the molar ratio of ~1:20). After 2 h of incubation with slow stirring at 4 °C, the sample was placed into the dialysis bag (12–14 kDa cutoff, Spectra/Por, VWR) in a container with 10 mL of buffer (50 mM KH_2PO_4, 300 mM NaCl, pH 7.5) and 8 g of Bio-beads SM-2 (Biorad). The sample was dialyzed for 7 days at 4 °C, changing the buffer every 24 h. The proteoliposome suspension was withdrawn from the dialysis bag and the proteoliposomes were collected by centrifugation at 300,000×*g* for 1 h at 4 °C. The pellet was washed several times by centrifugation at 300,000×*g* for 1 h at 4 °C in 10 mM NaCl, 25 mM Tris–HCl, pH 7, and the proteoliposomes were finally concentrated by ultra-centrifugation at 900,000×*g* for 9 h. The pellet obtained this way was ready for SSNMR rotor packing and kept at −20 °C until further use.

In order to verify the native fold, desired protein/lipid ratio, amount, and isotope labeling of hAQP1 in reconstituted samples, Fourier-transform infrared (FTIR) spectroscopy was employed. The proteoliposome pellets corresponding to ~0.05–0.2 mg of hAQP1 (taken before 900,000×*g* centrifugation step to avoid excessive aggregation) were resuspended in MilliQ water and dried on a CaF_2 window (Harrick). The dry film was covered by another CaF_2 window with a 6 micron Teflon spacer and placed in Bruker IFS66vs machine with a temperature-controlled sample holder (Harrick). Absorbance spectra were averages of 100 scans at 2 cm^{-1} resolution, with the spectra of two empty windows as a reference, the baseline distortions were corrected by OPUS software (Bruker). Figure 1 shows a representative FTIR spectrum of natural abundance hAQP1 taken in the mid-infrared range, containing protein backbone amide bands and lipid esters vibrations. The typical position and narrow linewidth of the Amide I band (at 1,657 cm^{-1}) agrees well with mainly α-helical structure of the protein, as previously determined by FTIR (Cabiaux et al. 1997) and crystallography (Murata et al. 2000; Ren et al. 2001; Sui et al. 2001). The ratio of the amplitudes of the Amide I band and the band corresponding to the lipid ester vibrations (at 1,738 cm^{-1}) (daCosta and Baenziger 2003) is consistent with the low lipid content (1/3 by weight) employed at the reconstitution step and suggests that no significant amount of yeast lipids was retained during purification. Upon isotope labeling, significant isotope shifts of the Amide I (upon ^{13}C labeling) and Amide II (upon ^{13}C and ^{15}N labeling) bands were observed (not shown).

To verify the functionality of hAQP1 in the lipids chosen for NMR experiments, we employed water permeability essays (Laize et al. 1997; Nyblom et al. 2007), mostly following the protocol for *S. cerevisiae*-expressed hAQP1 (Laize et al. 1997). As it is known that high protein content can make proteoliposomes leaky (Pitard et al. 1996b), the water permeability experiments had to be conducted at a substantially lower protein/lipid ratio (1/10 w/w) than that used for NMR experiments (2/1 w/w). Egg PC/Brain PS liposomes (9/1 molar ratio) were prepared by reverse-phase evaporation (Rigaud et al. 1983) and extruded through polycarbonate Isopore filters (0.4 and 0.2 microns) consecutively. The resulting liposome stock (15 mg/mL of lipids) was mixed with 0.2 mg/mL solution of purified hAQP1 in the imidazole-free elution buffer (1 % OG) to produce lipid/protein ratio of 10 (w/w), with addition of 0.8 % of Triton X-100 and 0.56 % of OG (Pitard et al. 1996a). After 2 h of incubation with slow stirring in 4 °C, the sample was placed in the dialysis bag in a container with 10 mL of buffer (150 mM KCl, 1 mM KH_2PO_4, pH 6.8) and 8 g of Bio-beads SM-2, and dialyzed for 48 h at 4 °C. As a control, the identical procedure was performed with protein-free liposomes, where addition of hAQP1 was replaced by the same volume of the buffer with 1 % OG. The proteoliposomes (and protein-free liposomes) were collected by centrifugation at 300,000×*g* for 1 h at 4 °C and resuspended in liposome buffer (20 mM Tris–HCl, pH 8.0, 150 mM NaCl) at 0.2 mg lipid/mL. Average diameter of the liposomes (170 nm) and proteoliposomes (179 nm) was estimated by Dynamic Light Scattering (Malvern Zetasizer). Water permeability measurements were performed using a stopped-flow spectrophotometer

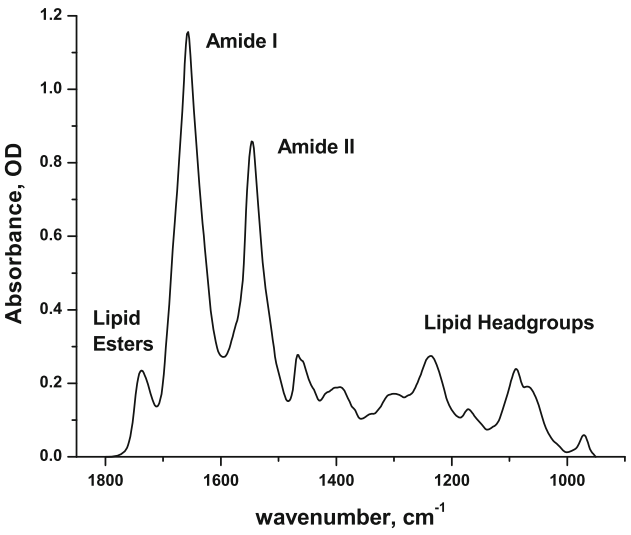

Fig. 1 FTIR absorbance spectrum of a dry film of natural abundance hAQP1 reconstituted in PC/PS liposomes at the protein/lipid ratio of 2 (w/w). Characteristic bands are labeled (see text for details)

(SX20, Applied Photophysics), by following kinetics of the increase in light scattering (at 480 nm) upon vesicles shrinking induced by hypertonic shock (180 mM sucrose at 22 °C), which reports on the rate of water efflux. The observed trends (Fig. 2) are very similar to those reported earlier (Laize et al. 1997; Nyblom et al. 2007), where hAQP1 proteoliposomes demonstrated much faster shrinking compared to the liposome controls. After the correction for the baseline drift (verified by mixing with isotonic solution lacking sucrose), the kinetics of water efflux from protein-free liposomes could be fitted by a single exponential with a characteristic time of 141 ± 3 ms, while that for the proteoliposomes was markedly biphasic (the major phase 23 ± 1 ms, 76 % of the amplitude, and the minor phase 197 ± 13 ms). Such a biphasic character for hAQP1 proteoliposomes was observed before and the slow kinetic phase was interpreted as corresponding to the protein-free population (Nyblom et al. 2007). An additional control was performed using specific inhibition of hAQP1 (achieved by a 15-min preincubation with 0.1 mM $HgCl_2$), which showed very significant suppression of the efflux (a single exponential with a characteristic time of 103 ± 1 ms). Such suppression was not observed upon the incubation of protein-free liposomes with $HgCl_2$ (not shown). Taken together, these data indicate that hAQP1 is functional in the PC/PS mixture employed in our study.

For the SSNMR measurements, the proteoliposomes were hydrated with 10 mM NaCl, 25 mM Tris–Cl, pH 7.0. The spectra were recorded on Bruker Avance III spectrometer operating at 800.23 MHz equipped with 3.2 mm E-free

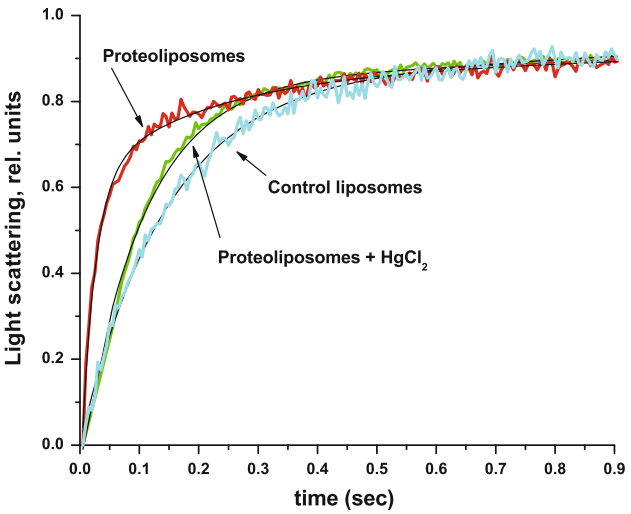

Fig. 2 Kinetics of the light scattering changes of PC/PS liposome suspensions upon hypertonic shock produced in the stopped-flow apparatus. Proteoliposomes reconstituted with hAQP1 (lipid/protein ratio of 10 w/w) are compared with protein-free liposomes and mercury-inhibited proteoliposomes. Each trace is an average of at least ten measurements. The exponential fits are shown with *black thin lines* (see text for details)

^{1}H–^{13}C–^{15}N probe (Bruker), the MAS frequency was 14.3 kHz. Hydrated proteoliposomes containing 6 mg of hAQP1 were center-packed in a thin-wall 3.2 mm rotor, and the sample temperature was maintained at 5 °C in all experiments. The obtained one-dimensional (1D) (Fig. 3) and two-dimensional (2D) (Figs. 4, 5) spectra show very good dispersion and excellent resolution (linewidths of ~0.5 ppm for carbon and ~0.5 ppm for nitrogen), which exceeds that demonstrated for microbial rhodopsins expressed both in *E. coli* and *P. pastoris* (Shi et al. 2009a, 2011; Fan et al. 2011). A large number of well-resolved narrow peaks belonging to side-chain and backbone atoms of various types of amino acids are identifiable in the spectra, which suggests that a very high level of chemical shift assignments should be possible from the future three-dimensional experiments, as recently demonstrated for *Anabaena* sensory rhodopsin (Wang et al. 2012). The sharpness of NMR peaks also suggests good sample homogeneity and, combined with the results of the functional assays (see above), gives hope that *Pichia*-expressed hAQP1 is fit for structural and functional studies by MAS SSNMR in the native-like lipid environment.

One-dimensional ^{15}N spectrum (Fig. 3a) shows a very good dispersion of the backbone signals, and also shows many peaks of Lys, Arg, and His side-chain atoms. One-dimensional ^{13}C spectrum (Fig. 3b) has equally high resolution and confirms the lack of glycosylation of hAQP1, as no sugar signals are observed in the 70–80 ppm range. Both ^{13}C–^{13}C (Fig. 4a) and NCA (Fig. 5) spectra allow identification of groups of peaks corresponding to intra-residue correlations of several amino acid types, such as Ala, Ser, and Thr in the former and Gly and Pro in the latter. It is possible to estimate the spectral coverage by counting well-resolved peaks of one type and estimating integrated intensity of the unresolved peaks. From our previous experience with microbial rhodopsins, we can expect that the peaks from residues in the transmembrane helices should be mostly visible, while those in the loops and tails may be weak (or even invisible) due to the unfavorable dynamics (Shi et al. 2009b; Fan et al. 2011). For example, we estimate that at least 18 Ala (out of the expected 22 TM and 8 extramembrane residues) and 20 Gly (out of the expected 18 TM and 9 extramembrane residues) are visible. Four Pro peaks are identifiable from the NCA spectra (there are 4 TM prolines), which should include the prolines of the functionally important conserved NPA motives in the water pore (Sui et al. 2001; Ren et al. 2001). As all of these Pro CA signals are found above 65 ppm, they must originate from the TM helices. Another interesting observation is that some peaks clearly correspond to non-helical conformations (Wang and Jardetzky 2002), such as those boxed in Fig. 4b, c for Ala and Ser/Thr, respectively. The CA/CB Ala resonances at around (51–52)/21 ppm (Fig. 4b) have chemical shifts close to

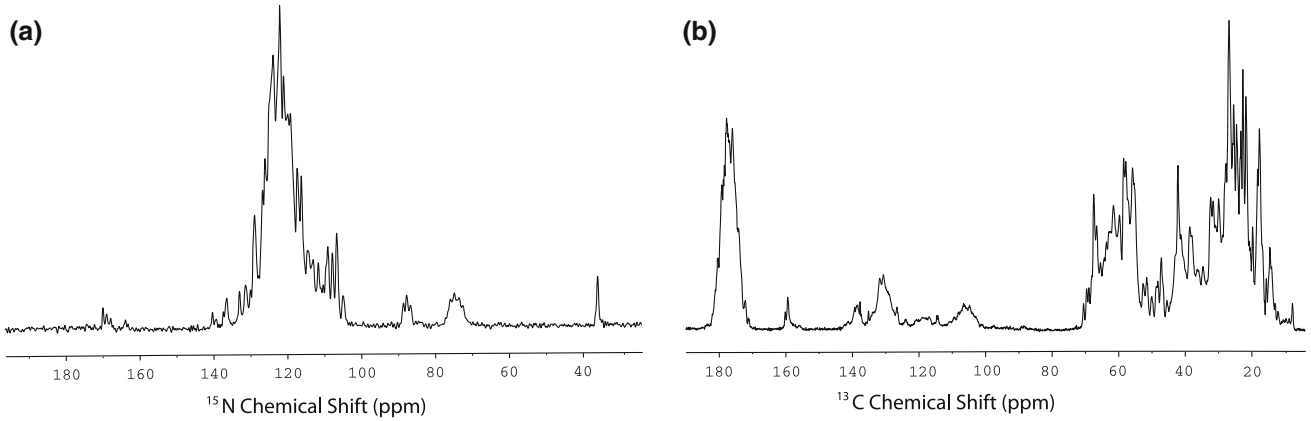

Fig. 3 One-dimensional ^{15}N (**a**) and ^{13}C (**b**) MAS NMR spectra of ^{13}C,^{15}N-labeled hAQP1 reconstituted in PC/PS liposomes recorded at 800 MHz, at 5 °C, and at a spinning rate of 14.3 kHz. ^{15}N spectrum was collected with 400 scans, and ^{13}C spectrum was averaged over 96 scans. SPINAL64 decoupling of 83 kHz was used during detection (Fung et al. 2000)

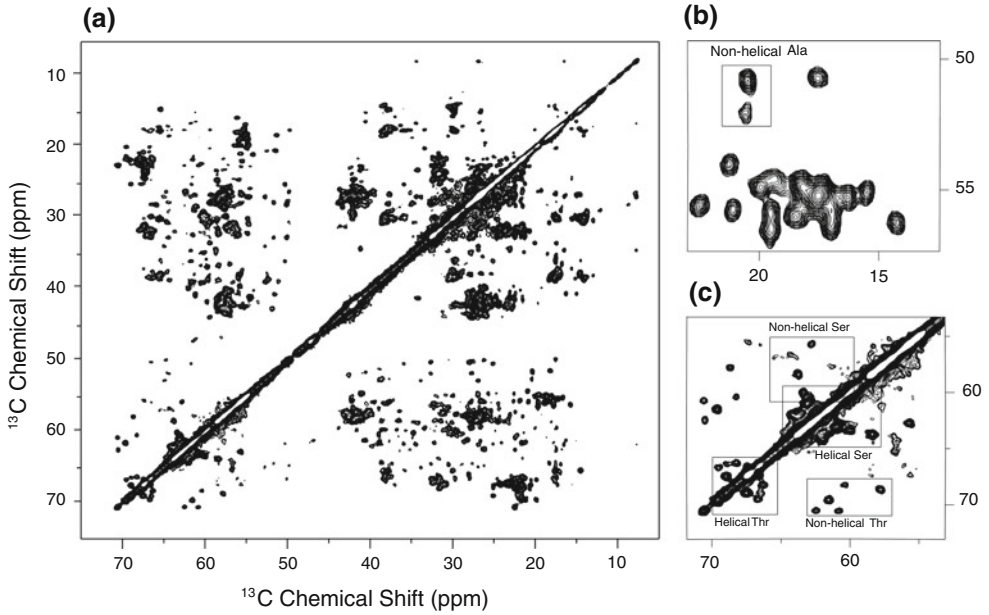

Fig. 4 **a** Two-dimensional ^{13}C–^{13}C DARR (Takegoshi et al. 2001) (dipolar assisted rotational resonance, also known as radiofrequency assisted diffusion (RAD) (Morcombe et al. 2004)) chemical shift correlation spectrum of ^{13}C,^{15}N-hAQP1 proteoliposomes at 800 MHz, at a spinning frequency of 14.3 kHz and at 5 °C. **b** Enlarged Ala Cα/Cβ region of the same spectrum. Residues showing non-helical conformations are boxed. **c** Enlarged Thr and Ser Cα/Cβ regions. Residues showing non-helical and helical conformations are boxed. The 2D spectrum was collected with 14.95 ms of the indirect t_1 acquisition with TPPI (time-proportional phase incrementation) (Marion and Wuthrich 1983) phase-sensitive detection, and 20.53 ms of the direct t_2 acquisition. 8 scans per point were collected with a recycle delay of 1.7 s. The total experimental time was 11 h. Data were processed with 40 Hz of Lorentzian line narrowing and 80 Hz of Gaussian line broadening in both dimensions. The first contour level is cut at 6 × σ, with each additional level multiplied by 1.1

those typical for β-strands, as do Ser resonances at (56–58)/(63–64) ppm and Thr resonances at (61–62)/70 ppm (Fig. 4c). As the available structures of human and bovine AQP do not show any β-strands, it is likely that these signals belong to the residues in β-turns, present according to FTIR (Cabiaux et al. 1997) and crystallographic studies (Murata et al. 2000; Ren et al. 2001; Sui et al. 2001; de Groot et al. 2001). In agreement with this, the Amide I band in the FTIR spectrum of hAQP1 shown in Fig. 1 displays a shoulder at 1,682 cm^{-1} (clearly seen as a peak in the second derivative of the spectrum, not shown). In the absence of the corresponding strong shoulder at ~1,630 cm^{-1} (signature of β-strands), this spectral feature can be safely interpreted as belonging to β-turns (Vass et al. 2003).

In summary, we demonstrated that expression and isotope labeling in *P. pastoris*, combined with functional reconstitution in native-like lipids, can produce samples of relatively

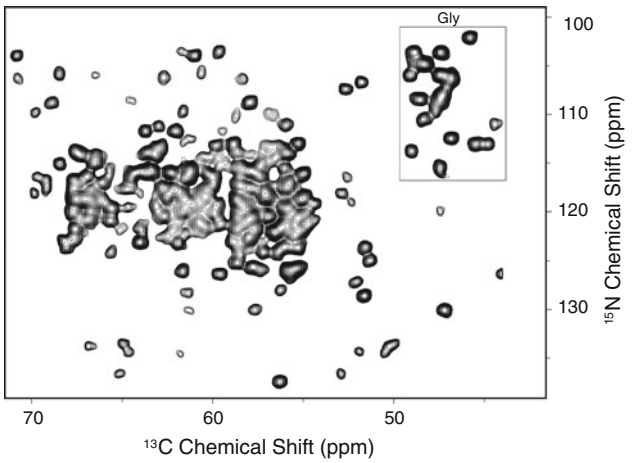

Fig. 5 Two-dimensional NCA spectrum of ^{13}C,^{15}N- hAQP1 proteoliposomes recorded at 800 MHz, at a spinning rate of 14.3 kHz, and at 5 °C. Glycine resonances are shown in the *box*. 2D spectrum was collected with 14.95 ms of the indirect t_1 acquisition with TPPI phase-sensitive detection, and with 20.53 ms of the direct t_2 acquisition. 24 scans per point were recorded with a recycle delay of 1.7 s. The total experiment time was 4 h. Data were processed with 40 Hz of Lorentzian line narrowing and 80 Hz of Gaussian line broadening in the CA direct dimension, and with 24 Hz of Lorentzian line narrowing and 40 Hz of Gaussian line broadening in the ^{15}N indirect dimension. The first contour is cut at $5 \times \sigma$, with each additional level multiplied by 1.2

large α-helical human membrane proteins suitable for multi-dimensional MAS SSNMR spectroscopy. These samples represent perfect targets for the in-depth structural and functional analyses, including those for mechanisms of interactions with pharmacological agents and other modulators.

Acknowledgments We thank Frederick Öberg and Kristina Hedfalk (Göteborg University, Sweden) for the generous gift of hAQP1 expression vector. The research was supported by the University of Guelph (start-up funds to V.L. and L.S.B.), the Natural Sciences and Engineering Research Council of Canada (discovery grants to L.S.B. and to V.L.), Canada Foundation for Innovation, and the Ontario Ministry of Research and Innovation. V.L. holds Canada Research Chair in biophysics, and S.E. is a recipient of the Ontario Trillium scholarship. We thank Drs. Armen Charchoglyan and Dyanne Brewer for MALDI-MS data collection. We thank Dr. Miguel Lugo for his help with stopped-flow measurements and Dr. Shenlin Wang for the help with NMR data processing. We thank Cambridge Isotope Laboratories for the generous gift of isotopically labeled methanol.

References

Agre P, King LS, Yasui M, Guggino WB, Ottersen OP, Fujiyoshi Y, Engel A, Nielsen S (2002) Aquaporin water channels—from atomic structure to clinical medicine. J Physiol 542:3–16

Ahuja S, Hornak V, Yan EC, Syrett N, Goncalves JA, Hirshfeld A, Ziliox M, Sakmar TP, Sheves M, Reeves PJ, Smith SO, Eilers M (2009) Helix movement is coupled to displacement of the second extracellular loop in rhodopsin activation. Nat Struct Mol Biol 16:168–175

Aller SG, Yu J, Ward A, Weng Y, Chittaboina S, Zhuo R, Harrell PM, Trinh YT, Zhang Q, Urbatsch IL, Chang G (2009) Structure of P-glycoprotein reveals a molecular basis for poly-specific drug binding. Science 323:1718–1722

Asada H, Uemura T, Yurugi-Kobayashi T, Shiroishi M, Shimamura T, Tsujimoto H, Ito K, Sugawara T, Nakane T, Nomura N, Murata T, Haga T, Iwata S, Kobayashi T (2011) Evaluation of the *Pichia pastoris* expression system for the production of GPCRs for structural analysis. Microb Cell Fact 10:24

Barnes AB, Paepe GD, van der Wel PC, Hu KN, Joo CG, Bajaj VS, Mak-Jurkauskas ML, Sirigiri JR, Herzfeld J, Temkin RJ, Griffin RG (2008) High-field dynamic nuclear polarization for solid and solution biological NMR. Appl Magn Reson 34:237–263

Berardi MJ, Shih WM, Harrison SC, Chou JJ (2011) Mitochondrial uncoupling protein 2 structure determined by NMR molecular fragment searching. Nature 476:109–113

Berger C, Ho JT, Kimura T, Hess S, Gawrisch K, Yeliseev A (2010) Preparation of stable isotope-labeled peripheral cannabinoid receptor CB2 by bacterial fermentation. Protein Expr Purif 70:236–247

Bornert O, Alkhalfioui F, Logez C, Wagner R (2012) Overexpression of membrane proteins using *Pichia pastoris*. Curr Protoc Protein Sci Chapter 29:29.2.1–29.2.24

Cabiaux V, Oberg KA, Pancoska P, Walz T, Agre P, Engel A (1997) Secondary structures comparison of aquaporin-1 and bacteriorhodopsin: a Fourier transform infrared spectroscopy study of two-dimensional membrane crystals. Biophys J 73:406–417

Chen H, Ilan B, Wu Y, Zhu F, Schulten K, Voth GA (2007) Charge delocalization in proton channels, I: the aquaporin channels and proton blockage. Biophys J 92:46–60

daCosta CJ, Baenziger JE (2003) A rapid method for assessing lipid:protein and detergent:protein ratios in membrane-protein crystallization. Acta Crystallogr 59:77–83

de Groot BL, Engel A, Grubmuller H (2001) A refined structure of human aquaporin-1. FEBS Lett 504:206–211

de Groot BL, Frigato T, Helms V, Grubmuller H (2003) The mechanism of proton exclusion in the aquaporin-1 water channel. J Mol Biol 333:279–293

Egorova-Zachernyuk TA, Bosman GJ, Degrip WJ (2011) Uniform stable-isotope labeling in mammalian cells: formulation of a cost-effective culture medium. Appl Microbiol Biotechnol 89:397–406

Fan Y, Shi L, Ladizhansky V, Brown LS (2011) Uniform isotope labeling of a eukaryotic seven-transmembrane helical protein in yeast enables high-resolution solid-state NMR studies in the lipid environment. J Biomol NMR 49:151–161

Fung BM, Khitrin AK, Ermolaev K (2000) An improved broadband decoupling sequence for liquid crystals and solids. J Magn Reson 142:97–101

Gautier A, Nietlispach D (2012) Solution NMR studies of integral polytopic alpha-helical membrane proteins: the structure determination of the seven-helix transmembrane receptor sensory rhodopsin II, pSRII. Methods Mol Biol (Clifton, NJ) 914:25–45

Goncalves JA, Ahuja S, Erfani S, Eilers M, Smith SO (2010) Structure and function of G protein-coupled receptors using NMR spectroscopy. Prog Nucl Magn Reson Spectrosc 57:159–180

Hiller S, Garces RG, Malia TJ, Orekhov VY, Colombini M, Wagner G (2008) Solution structure of the integral human membrane protein VDAC-1 in detergent micelles. Science 321:1206–1210

Hino T, Arakawa T, Iwanari H, Yurugi-Kobayashi T, Ikeda-Suno C, Nakada-Nakura Y, Kusano-Arai O, Weyand S, Shimamura T, Nomura N, Cameron AD, Kobayashi T, Hamakubo T, Iwata S, Murata T (2012) G-protein-coupled receptor inactivation by an allosteric inverse-agonist antibody. Nature 482:237–240

Ho JD, Yeh R, Sandstrom A, Chorny I, Harries WE, Robbins RA, Miercke LJ, Stroud RM (2009) Crystal structure of human

aquaporin 4 at 1.8 A and its mechanism of conductance. Proc Natl Acad Sci USA 106:7437–7442

Hong M, Zhang Y, Hu F (2012) Membrane protein structure and dynamics from NMR spectroscopy. Annu Rev Phys Chem 63:1–24

Horsefield R, Norden K, Fellert M, Backmark A, Tornroth-Horsefield S, van Terwisscha Scheltinga AC, Kvassman J, Kjellbom P, Johanson U, Neutze R (2008) High-resolution x-ray structure of human aquaporin 5. Proc Natl Acad Sci USA 105:13327–13332

Isaksson L, Enberg J, Neutze R, Goran Karlsson B, Pedersen A (2012) Expression screening of membrane proteins with cell-free protein synthesis. Protein Expr Purif 82:218–225

Issaly N, Solsona O, Joudrier P, Gautier MF, Moulin G, Boze H (2001) Optimization of the wheat puroindoline-a production in *Pichia pastoris*. J Appl Microbiol 90:397–406

Kim HJ, Howell SC, Van Horn WD, Jeon YH, Sanders CR (2009) Recent advances in the application of solution NMR spectroscopy to multi-span integral membrane proteins. Prog Nucl Magn Reson Spectrosc 55:335–360

Klammt C, Maslennikov I, Bayrhuber M, Eichmann C, Vajpai N, Chiu EJ, Blain KY, Esquivies L, Kwon JH, Balana B, Pieper U, Sali A, Slesinger PA, Kwiatkowski W, Riek R, Choe S (2012) Facile backbone structure determination of human membrane proteins by NMR spectroscopy. Nat Methods 9:834–839

Laize V, Ripoche P, Tacnet F (1997) Purification and functional reconstitution of the human CHIP28 water channel expressed in *Saccharomyces cerevisiae*. Protein Expr Purif 11:284–288

Li Y, Berthold DA, Gennis RB, Rienstra CM (2008) Chemical shift assignment of the transmembrane helices of DsbB, a 20-kDa integral membrane enzyme, by 3D magic-angle spinning NMR spectroscopy. Protein Sci 17:199–204

Long SB, Campbell EB, Mackinnon R (2005) Crystal structure of a mammalian voltage-dependent Shaker family K+ channel. Science 309:897–903

Lundstrom K, Wagner R, Reinhart C, Desmyter A, Cherouati N, Magnin T, Zeder-Lutz G, Courtot M, Prual C, Andre N, Hassaine G, Michel H, Cambillau C, Pattus F (2006) Structural genomics on membrane proteins: comparison of more than 100 GPCRs in 3 expression systems. J Struct Funct Genomics 7:77–91

Makino S, Goren MA, Fox BG, Markley JL (2010) Cell-free protein synthesis technology in NMR high-throughput structure determination. Methods Mol Biol (Clifton, NJ) 607:127–147

Marassi FM, Das BB, Lu GJ, Nothnagel HJ, Park SH, Son WS, Tian Y, Opella SJ (2011) Structure determination of membrane proteins in five easy pieces. Methods 55:363–369

Marion D, Wuthrich K (1983) Application of phase sensitive two-dimensional correlated spectroscopy (COSY) for measurements of 1H–1H spin–spin coupling constants in proteins. Biochem Biophys Res Commun 113:967–974

McDermott A (2009) Solid state NMR studies of enzymes and membrane proteins. Annu Rev Biophys 38:385–403

Morcombe CR, Gaponenko V, Byrd RA, Zilm KW (2004) Diluting abundant spins by isotope edited radio frequency field assisted diffusion. J Am Chem Soc 126:7196–7197

Morgan WD, Kragt A, Feeney J (2000) Expression of deuterium-isotope-labelled protein in the yeast *Pichia pastoris* for NMR studies. J Biomol NMR 17:337–347

Murata K, Mitsuoka K, Hirai T, Walz T, Agre P, Heymann JB, Engel A, Fujiyoshi Y (2000) Structural determinants of water permeation through aquaporin-1. Nature 407:599–605

Musa-Aziz R, Chen LM, Pelletier MF, Boron WF (2009) Relative CO_2/NH_3 selectivities of AQP1, AQP4, AQP5, AmtB, and RhAG. Proc Natl Acad Sci USA 106:5406–5411

Norden K, Agemark M, Danielson JA, Alexandersson E, Kjellbom P, Johanson U (2011) Increasing gene dosage greatly enhances recombinant expression of aquaporins in *Pichia pastoris*. BMC Biotechnol 11:47

Nyblom M, Oberg F, Lindkvist-Petersson K, Hallgren K, Findlay H, Wikstrom J, Karlsson A, Hansson O, Booth PJ, Bill RM, Neutze R, Hedfalk K (2007) Exceptional overproduction of a functional human membrane protein. Protein Expr Purif 56:110–120

Oberg F, Ekvall M, Nyblom M, Backmark A, Neutze R, Hedfalk K (2009) Insight into factors directing high production of eukaryotic membrane proteins; production of 13 human AQPs in *Pichia pastoris*. Mol Membr Biol 26:215–227

Oberg F, Sjohamn J, Conner MT, Bill RM, Hedfalk K (2011) Improving recombinant eukaryotic membrane protein yields in *Pichia pastoris*: the importance of codon optimization and clone selection. Mol Membr Biol 28:398–411

Park SH, Das BB, Casagrande F, Tian Y, Nothnagel HJ, Chu M, Kiefer H, Maier K, De Angelis AA, Marassi FM, Opella SJ (2012) Structure of the chemokine receptor CXCR1 in phospholipid bilayers. Nature 491:779–783

Pickford AR, O'Leary JM (2004) Isotopic labeling of recombinant proteins from the methylotrophic yeast *Pichia pastoris*. Methods Mol Biol (Clifton, NJ) 278:17–33

Pitard B, Richard P, Dunach M, Girault G, Rigaud JL (1996a) ATP synthesis by the F0F1 ATP synthase from thermophilic *Bacillus* PS3 reconstituted into liposomes with bacteriorhodopsin.1. Factors defining the optimal reconstitution of ATP synthases with bacteriorhodopsin. Eur J Biochem 235:769–778

Pitard B, Richard P, Dunach M, Rigaud JL (1996b) ATP synthesis by the F0F1 ATP synthase from thermophilic *Bacillus* PS3 reconstituted into liposomes with bacteriorhodopsin.2. Relationships between proton motive force and ATP synthesis. Eur J Biochem 235:779–788

Qureshi T, Goto NK (2012) Contemporary methods in structure determination of membrane proteins by solution NMR. Top Curr Chem 326:123–185

Ratnala VR (2006) New tools for G-protein coupled receptor (GPCR) drug discovery: combination of baculoviral expression system and solid state NMR. Biotechnol Lett 28:767–778

Reckel S, Sobhanifar S, Durst F, Lohr F, Shirokov VA, Dotsch V, Bernhard F (2010) Strategies for the cell-free expression of membrane proteins. Methods Mol Biol (Clifton, NJ) 607:187–212

Reckel S, Gottstein D, Stehle J, Lohr F, Verhoefen MK, Takeda M, Silvers R, Kainosho M, Glaubitz C, Wachtveitl J, Bernhard F, Schwalbe H, Guntert P, Dotsch V (2011) Solution NMR structure of proteorhodopsin. Angew Chem Int Ed Engl 50: 11942–11946

Ren G, Reddy VS, Cheng A, Melnyk P, Mitra AK (2001) Visualization of a water-selective pore by electron crystallography in vitreous ice. Proc Natl Acad Sci USA 98:1398–1403

Renault M, Cukkemane A, Baldus M (2010) Solid-state NMR spectroscopy on complex biomolecules. Angew Chem Int Ed Engl 49:8346–8357

Rigaud JL, Bluzat A, Buschlen S (1983) Incorporation of bacteriorhodopsin into large unilamellar liposomes by reverse phase evaporation. Biochem Biophys Res Commun 111:373–382

Rodriguez E, Krishna NR (2001) An economical method for (15)N/(13)C isotopic labeling of proteins expressed in *Pichia pastoris*. J Biochem 130:19–22

Seeliger D, Zapater C, Krenc D, Haddoub R, Flitsch S, Beitz E, Cerda J, de Groot BL (2012) Discovery of Novel Human Aquaporin-1 Blockers. ACS Chem Biol 8:249–256

Shi L, Ahmed MA, Zhang W, Whited G, Brown LS, Ladizhansky V (2009a) Three-dimensional solid-state NMR study of a seven-helical integral membrane proton pump structural insights. J Mol Biol 386:1078–1093

Shi L, Lake EM, Ahmed MA, Brown LS, Ladizhansky V (2009b) Solid-state NMR study of proteorhodopsin in the lipid

environment: secondary structure and dynamics. Biochim Biophys Acta 1788:2563–2574
Shi L, Kawamura I, Jung KH, Brown LS, Ladizhansky V (2011) Conformation of a seven-helical transmembrane photosensor in the lipid environment. Angew Chem Int Ed Engl 50:1302–1305
Shimamura T, Shiroishi M, Weyand S, Tsujimoto H, Winter G, Katritch V, Abagyan R, Cherezov V, Liu W, Han GW, Kobayashi T, Stevens RC, Iwata S (2011) Structure of the human histamine H1 receptor complex with doxepin. Nature 475:65–70
Singh S, Gras A, Fiez-Vandal C, Martinez M, Wagner R, Byrne B (2012) Large-scale production of membrane proteins in *Pichia pastoris*: the production of G protein-coupled receptors as a case study. Methods Mol Biol (Clifton, NJ) 866:197–207
Sugiki T, Ichikawa O, Miyazawa-Onami M, Shimada I, Takahashi H (2012) Isotopic labeling of heterologous proteins in the yeast *Pichia pastoris* and *Kluyveromyces lactis*. Methods Mol Biol (Clifton, NJ) 831:19–36
Sui H, Han BG, Lee JK, Walian P, Jap BK (2001) Structural basis of water-specific transport through the AQP1 water channel. Nature 414:872–878
Takahashi H, Shimada I (2010) Production of isotopically labeled heterologous proteins in non-*E. coli* prokaryotic and eukaryotic cells. J Biomol NMR 46:3–10
Takegoshi K, Nakamura S, Terao T (2001) C-13-H-1 dipolar-assisted rotational resonance in magic-angle spinning NMR. Chem Phys Lett 344:631–637
Tao X, Avalos JL, Chen J, MacKinnon R (2009) Crystal structure of the eukaryotic strong inward-rectifier K+ channel Kir2.2 at 3.1 A resolution. Science 326:1668–1674
Tapaneeyakorn S, Goddard AD, Oates J, Willis CL, Watts A (2011) Solution- and solid-state NMR studies of GPCRs and their ligands. Biochim Biophys Acta 1808:1462–1475
Vass E, Hollosi M, Besson F, Buchet R (2003) Vibrational spectroscopic detection of beta- and gamma-turns in synthetic and natural peptides and proteins. Chem Rev 103:1917–1954
Verardi R, Shi L, Traaseth NJ, Walsh N, Veglia G (2011) Structural topology of phospholamban pentamer in lipid bilayers by a hybrid solution and solid-state NMR method. Proc Natl Acad Sci USA 108:9101–9106
Wang Y, Jardetzky O (2002) Probability-based protein secondary structure identification using combined NMR chemical-shift data. Protein Sci 11:852–861
Wang S, Shi L, Okitsu T, Wada A, Brown LS, Ladizhansky V (2012) Solid-state NMR (13)C and (15)N resonance assignments of a seven-transmembrane helical protein Anabaena Sensory Rhodopsin. Biomol NMR Assign. doi:10.1007/s12104-012-9421-y
Warschawski DE, Arnold AA, Beaugrand M, Gravel A, Chartrand E, Marcotte I (2011) Choosing membrane mimetics for NMR structural studies of transmembrane proteins. Biochim Biophys Acta 1808:1957–1974
Waschuk SA, Bezerra AG, Shi L, Brown LS (2005) Leptosphaeria rhodopsin: bacteriorhodopsin-like proton pump from a eukaryote. P Natl Acad Sci USA 102:6879–6883
Werner K, Richter C, Klein-Seetharaman J, Schwalbe H (2008) Isotope labeling of mammalian GPCRs in HEK293 cells and characterization of the C-terminus of bovine rhodopsin by high resolution liquid NMR spectroscopy. J Biomol NMR 40:49–53
White SH (2009) Biophysical dissection of membrane proteins. Nature 459:344–346
Wood MJ, Komives EA (1999) Production of large quantities of isotopically labeled protein in *Pichia pastoris* by fermentation. J Biomol NMR 13:149–159
Yool AJ (2007) Functional domains of aquaporin-1: keys to physiology, and targets for drug discovery. Curr Pharm Des 13:3212–3221
Yool AJ, Brown EA, Flynn GA (2010) Roles for novel pharmacological blockers of aquaporins in the treatment of brain oedema and cancer. Clin Exp Pharmacol Physiol 37:403–409